

Application of $\text{CaTiO}_3:\text{Pr}^{3+}$ phosphor for enhancing the hue standard of WLEDs with double-film distant phosphor structure

Dieu An Nguyen Thi¹, Phan Xuan Le²

¹Faculty of Electrical Engineering Technology, Industrial University of Ho Chi Minh, Ho Chi Minh City, Viet Nam

²Faculty of Mechanical - Electrical and Computer Engineering, School of Engineering and Technology, Van Lang University, Ho Chi Minh City, Vietnam

Article Info

Article history:

Received Jul 23, 2021

Revised Sep 25, 2021

Accepted Nov 23, 2021

Keyword:

$\text{CaTiO}_3:\text{Pr}^{3+}$

Color quality scale

WLEDs

Luminous flux

Mie-scattering theory

ABSTRACT

Due to its great thermal stability, the WLEDs (short for white-light diodes), which are made of PiG (short for phosphor-in-glass), appear to be an optical source most effective at generating potent white illumination. However, the actual applications they offer are limited by their poor hue generation as well as hue uniformity. To improve these features, this study suggested utilizing a configuration involving a PiG-RPL (short for PiG integrated with a lens of phosphor in red). The phosphor YAGG (also known as $\text{Y}_3\text{Al}_3.08\text{Ga}_{1.92}\text{O}_{12}:\text{Ce}^{3+}$) and borosilicate glass powders were printed, then sintered to generate the green PiG, and then using an inverted dispensing approach, we applied the CASN phosphor silicone in red color (also known as $\text{CaAlSiN}_3:\text{Eu}^{2+}$) to the said PiG. As a result, with a current of 350 mA, the WLEDs made of PiG-RPL exhibit highly remarkable chromatic performance for the CRI (also known as color rendering index) values determined as $R_a = 95.6$ with $R_9 = 95.2$ and fidelity/gamut values determined as $R_f = 92$ with $R_g = 99.2$. The color quality of the PiG-RPL based WLED device would be steady over a wide range of currents (100 - 1000 mA). Moreover, PiG-RPL based WLEDs have better color uniformity than typical PiG based WLEDs.

Copyright © 2022 Institute of Advanced Engineering and Science.
All rights reserved.

Corresponding Author:

Phan Xuan Le

Faculty of Mechanical - Electrical and Computer Engineering, School of Engineering and Technology,

Van Lang University, Ho Chi Minh City, Vietnam

Email: le.px@vlu.edu.vn

1. INTRODUCTION

The term SSL (short for solid-state lighting) applies to the diodes that generate light (LEDs) owing to their great luminous efficiency, extended lifetime, environmentally friendly, and power savings [1-3]. Currently, pc-WLEDs, which stands for white LEDs made of conversion phosphors, are the most popular LEDs, which are made from a phosphor resin of yellow color activated via a chip of blue color in the LED. But the said resin appears to be susceptible to thermal aging due to inferior heat conductance and poor heat resistance [4, 5]. Under long light excitation, the thermal aging of phosphor-resin accelerates, lowering the light output in WLEDs. The inorganic chroma transmuters possessing great thermal endurance, such as PiG, phosphor ceramic, and independent crystal, have been introduced for pc-WLEDs to tackle this problem [6-8]. Because of its incomplex preparation, customizable luminescence, reasonable cost, and mass manufacture, the PiG would be considered practical as well as effective as a chroma transmuter. Originally, sintering a combination that includes YAG phosphors and glass powders at low temperatures created a yellow $\text{Y}_3\text{Al}_5\text{O}_{12}:\text{Ce}^{3+}$ (YAG) PiG, and then the composition are utilized to package WLEDs. Modifying the PiG's indexes, such as the proportion of phosphor-glass as well as the phosphor layer's thickness and arrangement, makes it simple to improve the light output in PiG-based WLEDs [9-11]. Unfortunately, when compared to natural light, the WLEDs made of YAG-phosphor PiG have low chromatic performance because of the

restricted emission spectra, which lack the spectrum of red and green color. To make multi-color PiGs, we included the portions of the green and red phosphors in the combination consisting of phosphor and glass so that we could improve the chromatic quality. Despite the fact that multi-color PiGs-based WLEDs have greater CRI value as well as smaller CCT (short for correlated color temperature), almost all WLEDs made of PiGs researched do not satisfy the specifications of great optical condition because the greatest CRI value is less than 90 with the ACU (short for angular color uniformity) shown to be relatively poor [12-15]. A cyan valley with the wavelength range of 470 nm to 500 nm within the WLEDs' emission spectra is thought to be the source of the CRI problem. Although several phosphors that generate cyan were developed to cover the imbalance of the cyan spectrum, they are unsuitable for sintering PiG due to their severe chemical and thermal deterioration. A phosphor of green color with wide band was placed to the combination of phosphor-glass of red color to produce a wide-band PiG with no cyan valley due to the green phosphor [16]. Nonetheless, during the sintering process, almost all phosphors of red color undergo interfacial reactivity along with heat failure, leading to reduced LE (short for lumen efficiency) in such WLED devices. In addition, the flat PiG construction causes a significant divergence in CCT level under all angles of viewing, reducing the optical effectiveness. Therefore, a green PiG covered with a phosphor lens in red (PiG-RPL) was recommended for the purpose of improving chromatic generation as well as homogeneity in WLED devices in this paper.

2. RESEARCH METHOD

2.1. Preparation

The phosphor composition of the red phosphor $\text{CaTiO}_3:\text{Pr}^{3+}$ is critical components of this study. To obtain the greatest phosphor films which can deliver the right consequences, the phosphor substance must be prepared carefully. The ingredients of red $\text{CaTiO}_3:\text{Pr}^{3+}$ phosphor are listed in Table 1 [17, 18]. This phosphor is obtained by a two-step firing procedure. To generate a uniform mixture, all of the ingredients must be slurried in methanol and dried in the air. When dry, the mixture is powdered before beginning the first firing stage. Next, at 1300°C , burn this combination in open quartz boats in 1 hour. Then remove the mixture and powder it by grinding or milling. The second step of fire follows. The powdered product is fired again with the same procedure and temperature. After this stage, the material is done whose emission peak is 2.025 eV and full-width at half-maximum (FWHM) is 0.05 eV. The $\text{CaTiO}_3:\text{Pr}^{3+}$ phosphor's stimulation effectiveness by UV is + (4.88 eV), + (3.40 eV).

Table 1. Components for creating the red-light $\text{CaTiO}_3:\text{Pr}^{3+}$ phosphor

Ingredients	Mole %	By weight (g)
CaCO_3	100	100
Pr_2O_3	1	1.64
TiO_2	100	80

2.2. Simulation

In this study, in order to build the LED simulation, the LightTools software along with the theory of Mie-scattering must be used, and the accuracy of the findings must be double-checked [19-21]. After all of the data on the scattering properties of phosphor particles used to support research on the influence of phosphorus $\text{Ca}_5\text{B}_2\text{SiO}_{10}:\text{Eu}^{3+}$ on WLED at a high correlation temperature of 5600K has been gathered, it is indeed necessary to simulate WLEDs with double-layer phosphorus. The generation of the $\text{CaTiO}_3:\text{Pr}^{3+}$ and $\text{YAG}:\text{Ce}^{3+}$ phosphor compound to construct the in-cup phosphor layout in WLEDs is shown by Figure 1. According to the figure, the order of the phosphor sheets appears as follows: the phosphor $\text{CaTiO}_3:\text{Pr}^{3+}$, the yellow phosphor $\text{YAG}:\text{Ce}^{3+}$, with silicone glues. The chips in blue color, a reflector dome, the sheets of phosphor, and a sheet of silicone make up the WLEDs model I Figure 1. The reflector that covers the chips is 2.07 mm deep, with bottom determined to be 8 mm long, and top surface being 9.85 mm long. At 453 nm as peak wavelength, each of the 9 blue chips possesses emitting energy measured at 1.16 W. $\text{CaTiO}_3:\text{Pr}^{3+}$ phosphor has a refractive index of 1.85, while that of $\text{YAG}:\text{Ce}^{3+}$ is 1.83. To balance the variation of $\text{CaTiO}_3:\text{Pr}^{3+}$ concentration as well as to maintain average CCTs, the $\text{YAG}:\text{Ce}^{3+}$ concentration must be adjusted suitably.

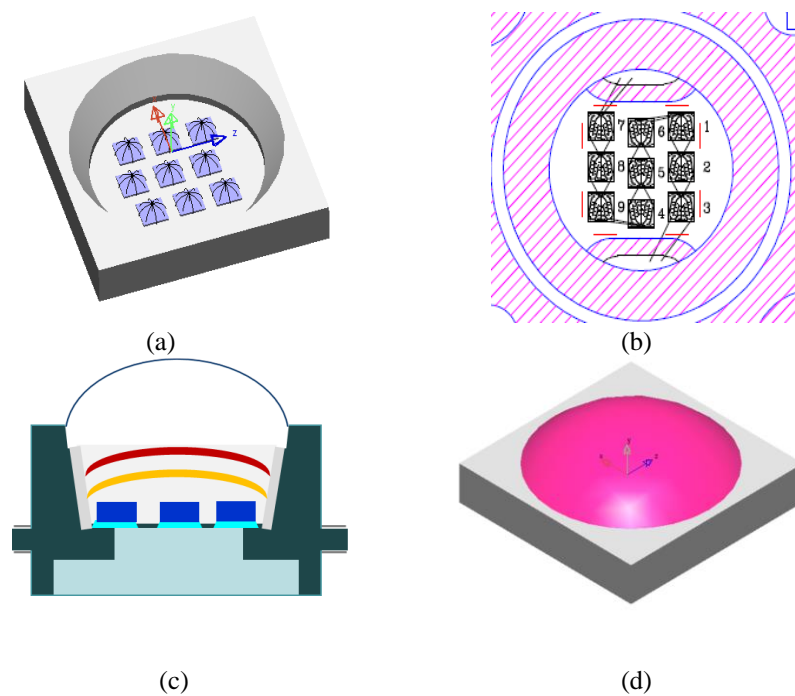


Figure 1. (a) 3D modeling, (b) Binding graph, (c) model of pc-WLEDs cross-section, (d) illustration of WLEDs simulated from LightTools commercial application

3. RESULTS AND DISCUSSION

Figure 2 shows the variation of YAG:Ce³⁺ phosphor sustaining the standard CCT levels as phosphor CaTiO₃:Pr³⁺ increases. For example, as the concentration of CaTiO₃:Pr³⁺ grows in the range of 2% to 26% wt., the YAG:Ce³⁺ phosphor concentration must reduce to preserve the standard CCT, which is true for WLEDs at 5600K. The scattering and absorption qualities are also impacted by the variation based on these findings, which potentially enhances the chromatic performance as well as light result in WLED devices. Subsequently, the CaTiO₃:Pr³⁺ phosphor concentration is critical, as this phosphor determines the performance of WLEDs.

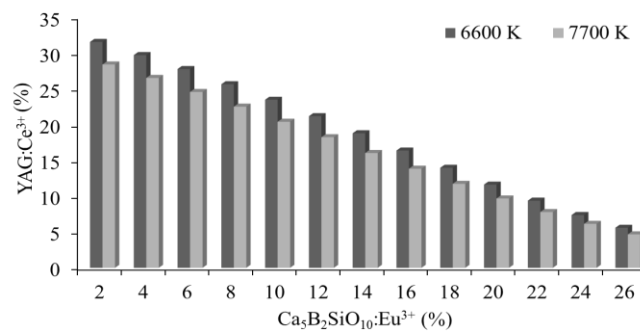


Figure 2. The equilibrium among two phosphor concentrations to maintain the average CCT

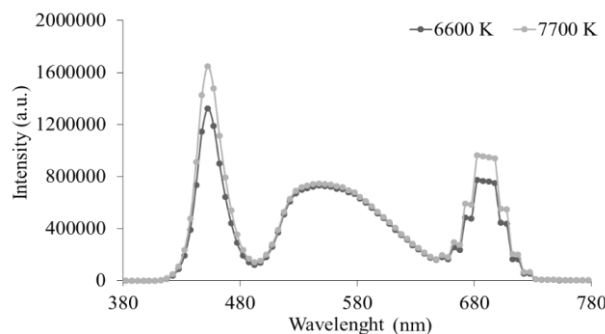


Figure 3. The emission spectra of WLEDs corresponding to $\text{CaTiO}_3:\text{Pr}^{3+}$ concentration

The effects of red phosphor $\text{CaTiO}_3:\text{Pr}^{3+}$ in concentrations of 2% and 24% applying to the emission spectrum in WLED devices are shown by Figure 3. When the luminous flux of a WLED is set to 5600K ACCT, the spectral regions produce white light. The red circle expands with three different concentrations of $\text{CaTiO}_3:\text{Pr}^{3+}$ the most significant of which is from 648 to 738 nm, followed by 420-480 nm and 500-640 nm. The quality will be improved if the scattered blue light occurs in the 420nm - 480nm emission spectrum. The color temperature affects the expansion for the emission spectrum. The findings show that the inclusion of $\text{CaTiO}_3:\text{Pr}^{3+}$ at low (6600 K) as well as great (7700 K) color temperatures will improve the color quality in WLEDs significantly. This is an important finding that has an impact on how manufacturers choose the optimum concentration to make the most efficient LEDs. The lumen output in these WLED devices is a minor drawback in WLED devices having good chromatic performance that manufacturers need to be aware of.

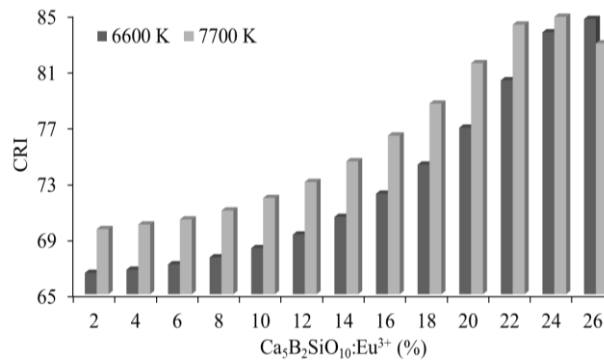


Figure 4. The WLEDs' CRI values with respective concentration of $\text{Ca}_5\text{B}_2\text{SiO}_{10}:\text{Eu}^{3+}$

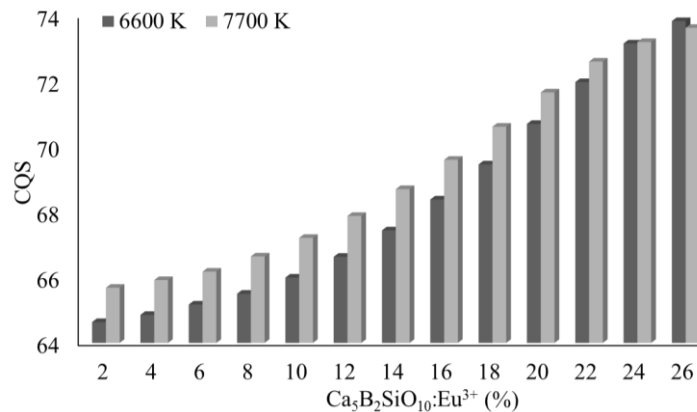


Figure 5. The WLEDs' CQS values (short for color quality scale) with respective concentration of $\text{Ca}_5\text{B}_2\text{SiO}_{10}:\text{Eu}^{3+}$

With the absorption attribute of the $\text{CaTiO}_3:\text{Pr}^{3+}$ phosphor in red, the outcomes in Figure 4 imply that adding $\text{CaTiO}_3:\text{Pr}^{3+}$ phosphor can raise the color rendering index and absorb more blue light than yellow. As a result, the red phosphor $\text{CaTiO}_3:\text{Pr}^{3+}$ increases the element that generates red light within WLED devices, and as a result becomes favorable for the CRI. The CRI parameter proves to be among the most important detail for assessing a WLED efficacy; the greater the CRI, the greater the WLED performance, and hence the more the expenses. Owing to the low cost of $\text{CaTiO}_3:\text{Pr}^{3+}$ phosphor, WLEDs with $\text{CaTiO}_3:\text{Pr}^{3+}$ phosphor will be utilized more frequently. Because CRI is not a very in-depth indicator, it is no longer significant for evaluating the color quality of WLEDs. Alternatively, the CQS is considered a more precise and effective measure to assess the effectiveness of WLEDs. CQS is now the most accurate color quality index, as it can evaluate three elements of WLEDs: CRI, beholder's taste, and chromatic coordinates. Figure 5 depicts the effect on the CQS of the red phosphor $\text{CaTiO}_3:\text{Pr}^{3+}$, demonstrating the improvement in hue standard. Although the $\text{CaTiO}_3:\text{Pr}^{3+}$ phosphor improves hue standard, the proportion of released illumination lowered by this phosphor cannot be overlooked. In the next section, we'll look at an equation demonstrating the propagated blue light and transmuted yellow illumination of the two-film phosphor layout, which could help boost the effectiveness of the LED device:

A Gaussian function is commonly used to describe the asymmetrical spectral energy allocation (SPD) in monochromatic LEDs [22, 23]:

$$P_\lambda = P_{opt} \frac{1}{\sigma\sqrt{2\pi}} \exp \exp \left[-0.5 * \frac{(\lambda - \lambda_{peak})^2}{\sigma^2} \right] \quad (1)$$

σ is decided by the peak wavelength λ_{peak} and FWHM $\Delta\lambda$ is determined as follow:

$$\sigma = \frac{\lambda_{peak}^2 \Delta E}{2hc\sqrt{2\ln 2}} = \frac{\lambda_{peak}^2 \left(\frac{hc}{\lambda_1} - \frac{hc}{\lambda_2} \right)}{2hc\sqrt{2\ln 2}} = \frac{\lambda_{peak}^2 \left(\frac{hc\Delta\lambda}{\lambda_1\lambda_2} \right)}{2hc\sqrt{2\ln 2}} \quad (2)$$

The accumulation of the spectrum in yellow and blue color can theoretically be interpreted as the WLED device's SPD using phosphor YAG in yellow color and a chip of LED in blue color. In practice, however, the stated yellow phosphor illuminates with green and yellow wavelengths (demonstrated by the deliberate spectrum of Figures 1 and 2). If we select ranges in yellow and blue hues, the disparity between the predicted SPD and twofold shading (yellow and blue shading) range model can be addressed to by a green range. As a result, to speak to the actual scenario, we may include a green range in the design with two ranges, resulting in the exploratory trispectrum (B–G–Y) model (3), which can then be changed as (4).

$$\begin{aligned} P_\lambda = & P_{opt_b} \frac{1}{\sigma_b\sqrt{2\pi}} \exp \exp \left[-0.5 * \frac{(\lambda - \lambda_{peak_b})^2}{\sigma_b^2} \right] \\ & + P_{opt_g} \frac{1}{\sigma_g\sqrt{2\pi}} \exp \exp \left[-0.5 * \frac{(\lambda - \lambda_{peak_g})^2}{\sigma_g^2} \right] \\ & + P_{opt_y} \frac{1}{\sigma_y\sqrt{2\pi}} \exp \exp \left[-0.5 * \frac{(\lambda - \lambda_{peak_y})^2}{\sigma_y^2} \right] \end{aligned} \quad (3)$$

$$\begin{aligned} P_\lambda = & \eta_b P_{opt_total} \frac{1}{\sigma_b\sqrt{2\pi}} \exp \exp \left[-0.5 * \frac{(\lambda - \lambda_{peak_b})^2}{\sigma_b^2} \right] \\ & + \eta_g P_{opt_total} \frac{1}{\sigma_g\sqrt{2\pi}} \exp \exp \left[-0.5 * \frac{(\lambda - \lambda_{peak_g})^2}{\sigma_g^2} \right] \\ & + \eta_y P_{opt_total} \frac{1}{\sigma_y\sqrt{2\pi}} \exp \exp \left[-0.5 * \frac{(\lambda - \lambda_{peak_y})^2}{\sigma_y^2} \right] \end{aligned} \quad (4)$$

For the equations demonstrated:

- P_λ Spectral power distribution (mW/nm).
- h Planck's constant (J.s).
- c Speed of light ($m \cdot s^{-1}$).
- λ Wavelength (nm).
- P_{opt} Optical power (W).
- λ_{peak} Peak wavelength (nm).
- $\Delta\lambda$ Full-width at half-maximum (nm).
- η Ratio of specific spectra to white spectrum, dimensionless.
- P_{opt_g} , P_{opt_b} , P_{opt_y} , and P_{opt_total} Optical power (W) for the green, blue, yellow, and white spectra, respectively.
- λ_{peak_g} , λ_{peak_b} , and λ_{peak_y} Peak wavelengths (nm) for the green, blue, and yellow spectra, respectively.
- σ_g , σ_b , and σ_y FWHM-related coefficients (nm) for the green, blue, and yellow spectra, respectively.
- η_b , η_b , and η_y Ratios of green–blue–yellow (G–B–Y) spectra to white spectrum, respectively, dimensionless.
- λ_1 , λ_2 Wavelengths at half of the peak intensity.

As a result, SPD designed for WLED devices treated with phosphor, which is thought of as an enhanced Gaussian model, can be stated as a tricolor spectrum. We utilize Mie-theory to examine the scattering of $\text{CaTiO}_3:\text{Pr}^{3+}$ phosphor particles. Furthermore, with the theory of Mie-scattering [24], the diffusing cross-section C_{sca} of globular granules will be identified via the equation below. The law of Lambert-Beer [25] can be utilized to determine the propagated optical energy:

$$I = I_0 \exp(-\mu_{ext}L) \quad (5)$$

For the demonstrated equation, I_0 denotes incident light power, L denotes the phosphor sheet's breadth in millimeters, μ_{ext} denotes the extinction coefficient, which could be derived using the following equation: $\mu_{ext} = N_r \cdot C_{ext}$, with N_r being the granules' number density dispensation (measured in mm^{-3}), and C_{ext} (measured in mm^2) being the extinction cross-section for phosphor granules. The result of applying Expression (5) reveals that a two-layer remote phosphor layout produces significantly more lumen when compared to a one-layer phosphor layout, see Figure 6. Subsequently, the two-layer phosphor layout contributes to a boost in lumen of WLED devices. The concentration of $\text{CaTiO}_3:\text{Pr}^{3+}$ remarkably influences the light output in double-layer phosphor structure WLEDs with red phosphor $\text{CaTiO}_3:\text{Pr}^{3+}$. The Lambert-Beer law shows that the extinction coefficient μ_{ext} and the concentration of $\text{CaTiO}_3:\text{Pr}^{3+}$ rise in sync; but the power of light emission increases in the opposite manner compared to the extinction factor μ_{ext} . As a consequence, raising the phosphor layers' breadth by having extra $\text{CaTiO}_3:\text{Pr}^{3+}$, can reduce the luminous flux of WLEDs. Figure 10 illustrates this conclusion by showing diminishing luminous fluxes in all CCTs as the $\text{CaTiO}_3:\text{Pr}^{3+}$ concentration rises to 26%. In general, adopting a double-layer phosphor layout made of the $\text{CaTiO}_3:\text{Pr}^{3+}$ phosphor in red produced significantly greater lumen when compared to a one-layer layout, and $\text{CaTiO}_3:\text{Pr}^{3+}$ also provides numerous CRI and CQS improvements. As a result, an insignificant loss of lumen output appears to be only a small concern in terms of the benefits. The most appropriate concentration setting is determined by the producer; the optimal concentration of $\text{CaTiO}_3:\text{Pr}^{3+}$ can correspond with their quality demands in the mass production of WLEDs.

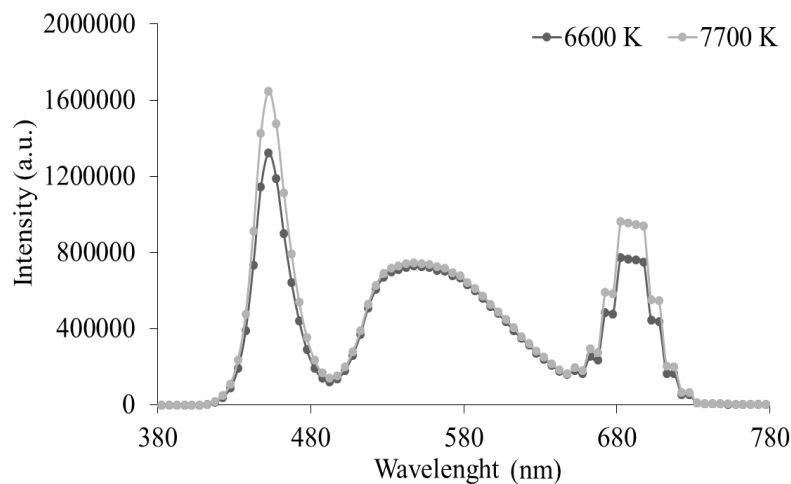


Figure 6. The WLED devices' lumen with respective concentration of $\text{CaTiO}_3:\text{Pr}^{3+}$

4. CONCLUSION

The WLEDs (short for white-light diodes) made of PiG become an optical source most effective at generating potent white illumination because of the excellent heat consistency. Besides, because of their poor chromatic generation as well as homogeneity, their practical uses are limited. Our research presented a configuration involving a PiG-RPL (short for PiG integrated with a lens of red phosphor) in order to increase chromatic generation as well as homogeneity. After the phosphor YAGG (also known as $\text{Y}_3\text{Al}_3.08\text{Ga}_{1.92}\text{O}_{12}:\text{Ce}^{3+}$) and borosilicate glass powders were printed, then sintered, we obtained the green PiG which was then covered by the CASN phosphor silicone in red color (also known as $\text{CaAlSiN}_3:\text{Eu}^{2+}$) using the reversed distribution technique. The outcome shows that the WLED devices made of PiG-RPL feature remarkable chromatic performance for CRIs (short for color rendering index) determined as $R_a = 95.6$ with $R_9 = 95.2$ and fidelity/gamut indexes determined as $R_f = 92$ with $R_g = 99.2$) under amperage measured at 350 milliamperes. The color quality of WLED devices made of PiG-RPL remains consistent over a wide current range of 100 - 1000 mA. PiG-RPL based WLEDs also have superior color uniformity than conventional PiG-based WLEDs. PiG-RPL-based WLEDs also have superior color uniformity than PiG-based WLEDs. This work proposes the layout of PiG-RPL to improve chromatic generation as well as homogeneity in WLED devices. We created the PiGRPL through using a green YAGG PiG on a lens of CASN phosphor in red. The said layout provides extremely excellent color rendering for WLEDs. Furthermore, color uniformity is better in WLED devices made of PiG-RPL when compared to WLED devices made of PiG and PiG-RPP. The PiG-RPL color converters are predicted to perform well in high-power WLEDs, with excellent color rendering and uniformity.

ACKNOWLEDGEMENTS

This study was financially supported by Van Lang University, Vietnam.

REFERENCES

- [1] S. Sadeghi, B. G. Kumar, R. Melikov, M. M. Aria, H. B. Jalali, and S. Nizamoglu, "Quantum dot white LEDs with high luminous efficiency," *Optica*, vol. 5, pp. 793-802, 2018, doi: 10.1364/OPTICA.5.000793.
- [2] X. Kong, M. Wei, M. J. Murdoch, I. Vogels, and I. Heynderickx, "Assessing the temporal uniformity of CIELAB hue angle," *J. Opt. Soc. Am. A*, vol. 37, pp. 521-528, 2020, doi: 10.1364/JOSAA.384393.
- [3] Z. Whenting, J. Liu, D. Hua, S. Guo, K. Yan, and C. Zhang, "White LED light source radar system for multi-wavelength remote sensing measurement of atmospheric aerosols", *Applied Optics*, vol. 58(31), pp. 8542-8548, 2019, doi: 10.1364/AO.58.008542.
- [4] Z. Yingjun, Y. Wei, F. Hu, J. Hu, Y. Zhao, J. Zhang, F. Jiang, and N. Chi, "Comparison of nonlinear equalizers for high-speed visible light communication utilizing silicon substrate phosphorescent white LED", *Optics Express*, vol. 28(2), pp. 2302-2316, 2020, doi: 10.1364/OE.383775.
- [5] T. Marco, and G. Zibordi, "Spatial uniformity of the spectral radiance by white LED-based flat-fields", *OSA Continuum*, vol. 3(9), pp. 2501-2511, 2020, doi: 10.1364/OSAC.394805.
- [6] X. Xiaoqian, L. Zhang, J. Kang, Y. Li, Z. Wang, B. Fei, X. Cheng, G. Huang, M. Li, and H. Chen, "Chip-level Ce:GdYAG ceramic phosphors with excellent chromaticity parameters for high-brightness white LED device", *Optics Express*, vol. 29(8), pp. 11938-11946, 2021, doi: 10.1364/OE.416486.
- [7] Z. Guozhao, K. Ding, G. He, and P. Zhong, "Spectral optimization of color temperature tunable white LEDs with red LEDs instead of phosphor for an excellent IES color fidelity index", *OSA Continuum*, vol. 2(4), pp. 1056-1064, 2019, doi: 10.1364/OSAC.2.001056.
- [8] M. Yuelong, L. Zhang, J. Huang, R. Wang, T. Li, T. Zhou, Z. Shi, J. W. Li, Y. Li, G. Huang, Z. Wang, F. A. Selim, M. Li, Y. Wang, and H. Chen, "Broadband emission Gd3Sc2Al3O12:Ce3+ transparent ceramics with a high color rendering index for high-power white LEDs/LDs", *Optics Express*, vol. 29(6), pp. 9474-9493, 2021, doi: 10.1364/OE.417464.
- [9] B. Shuvamoy, K. Annapurna, and A. Tarafder, "Realization of phosphor-in-glass thin film on soda-lime silicate glass with low sintering temperature for high color rendering white LEDs", *Applied Optics*, vol. 58(9), pp. 2372-2381, 2019, doi: 10.1364/AO.58.002372.
- [10] S. V. Cent, and C. C. Gao, "Remote GaN metalens applied to white light-emitting diodes", *Optics Express*, vol. 28(26), pp. 38883-38891, 2020, doi: 10.1364/OE.411525.
- [11] S. H. Kun, C. N. Liu, W. C. Cheng, and W. H. Cheng, "High color rendering index of 94 in white LEDs employing novel CaAlSiN3: Eu2+ and Lu3Al5O12: Ce3+ co-doped phosphor-in-glass", *Optics Express*, vol. 28(19), pp. 28218-28225, 2020, doi: 10.1364/OE.403410.
- [12] X. G. Y. Ma, X. Chen, S. Q. Jin, and C. Huang, "Comparison of MAP method with classical methods for bandpass correction of white LED spectra", *Journal of the Optical Society of America A*, vol. 36(5), pp. 751-758, 2019, doi: 10.1364/JOSAA.36.000751.
- [13] Y. Hurriyet, T. Guner, S. Balci, and M. M. Demir, "Phosphor-based white LED by various glassy particles: control over luminous efficiency", *Optics Letters*, vol. 44(3), pp. 479-482, 2019, doi: 10.1364/OL.44.000479.
- [14] Y. Xing, C. Chai, J. Chen, S. Zheng, and C. Chen, "Single 395 nm excitation warm WLED with a luminous efficiency of 104.86 lm/W and a color rendering index of 90.7", *Optical Materials Express*, vol. 9(11), pp. 4273-4286, 2019, doi: 10.1364/OME.9.004273.
- [15] L. Hongjian, P. Li, H. Zhang, Y. C. Chow, M. S. Wong, S. Pinna, J. Klamkin, J. S. Speck, S. Nakamura, and S. P. DenBaars, "Electrically driven, polarized, phosphor-free white semipolar (20-21) InGaN light-emitting diodes grown on semipolar bulk GaN substrate", *Optics Express*, vol. 28(9), pp. 13569-13575, 2020, doi: 10.1364/OE.384139.
- [16] Z. Tanglei, X. Zhang, B. Ding, J. Shen, Y. Hu, and H. Gu, "Homo-epitaxial secondary growth of ZnO nanowire arrays for a UV-free warm white light-emitting diode application", *Applied Optics*, vol. 59(8), pp. 2498-2504, 2020, doi: 10.1364/AO.385656.
- [17] J. Yung-Chang, X. H. Lee, S. K. Lin, C. C. Sun, C. S. Wu, Y. W. Yu, and T. H. Yang, "Design of an energy-efficient marine signal light based on white LEDs", *OSA Continuum*, vol. 2(8), pp. 2460-2469, 2019, doi: 10.1364/OSAC.2.002460.
- [18] L. C. Hao, A. Verma, C. Y. Kang, Y. M. Pai, T. Y. Chen, J. J. Yang, C. W. Sher, Y. Z. Yang, P. T. Lee, C. C. Lin, Y. C. Wu, S. K. Sharma, T. Wu, S. R. Chung, and H. C. Kuo, "Hybrid-type white LEDs based on inorganic halide perovskite QDs: candidates for wide color gamut display backlights", *Photonics Research*, vol. 7(5), pp. 579-585, 2019, doi: 10.1364/PRJ.7.000579.
- [19] L. Zongtao, J. Zheng, J. Li, W. Zhan, and Y. Tang, "Efficiency enhancement of quantum dot-phosphor hybrid white-light-emitting diodes using a centrifugation-based quasi-horizontal separation structure", *Optics Express*, vol. 28(9), pp. 13279-13289, 2020, doi: 10.1364/OE.392900.
- [20] T. D. Thi, V. T. H. Quan, B. Bondzior, P. J. Dereń, R. T. Velpula, H. P. T. Nguyen, L. A. Tuyen, N. Q. Hung, and H. D. Nguyen, "Deep red fluoride dots-in-nanoparticles for high color quality micro white light-emitting diodes", *Optics Express*, vol. 28(18), pp. 26189-26199, 2020, doi: 10.1364/OE.400848.
- [21] N. D. Q. Anh, P. X. Le, and H. Y. Lee, "Selection of a Remote Phosphor Configuration to Enhance the Color Quality of White LEDs", *Current Optics and Photonics*, vol. 3(1), pp. 78-85, 2019, doi: 10.3807/COPP.2019.3.1.078.

- [22] K. O. Hyeon, J. S. Kim, J. W. Jang, and Y. S. Cho, "Simple prismatic patterning approach for nearly room-temperature processed planar remote phosphor layers for enhanced white luminescence efficiency", *Optical Materials Express*, vol. 8(10), pp. 3230-3237, 2018, doi: 10.1364/OME.8.003230.
- [23] J. S. Wook, S. Kim, J. Choi, I. Jang, Y. Song, W. H. Kim, and J. P. Kim, "Optical design of dental light using a remote phosphor light-emitting diode package for improving illumination uniformity", *Applied Optics*, vol. 57(21), pp. 5998-6003, 2018, doi: 10.1364/AO.57.005998.
- [24] Y. Hurriyet, T. Guner, S. Balci, and M. M. Demir, "Phosphor-based white LED by various glassy particles: control over luminous efficiency", *Optics Letters*, vol. 44(3), pp. 479-482, 2019, doi: 10.1364/OL.44.000479.
- [25] Z. Zhili, H. Zhang, S. Liu, and X. Wang, "Effective freeform TIR lens designed for LEDs with high angular color uniformity", *Applied Optics*, vol. 57(15), pp. 4216-4221, 2018, doi: 10.1364/AO.57.004216.

BIOGRAPHIES OF AUTHORS



Dieu An Nguyen Thi received a master of Electrical Engineering, HCMC University of Technology and Education, VietNam. Currently, she is a lecturer at the Faculty of Electrical Engineering Technology, Industrial University of Ho Chi Minh City, Viet Nam. Her research interests are Theoretical Physics and Mathematical Physics. She can be contacted at email: nguyenthidieuan@iuh.edu.vn.

ORCID: 0000-0002-5327-1002




Scopus: Dieu An Nguyen nguyenthidieuan@iuh.edu.vn.

Google Scholar:

https://scholar.google.com/citations?view_op=list_works&hl=vi&user=qNwCM0oAAAAJ

Publons: <https://publons.com/researcher/4954208/nguyen-thi-dieu-an/>



Phan Xuan Le    received a Ph.D. in Mechanical and Electrical Engineering from Kunming University of Science and Technology, Kunming city, Yunnan province, China. Currently, He is a lecturer at the Faculty of Engineering, Van Lang University, Ho Chi Minh City, Viet Nam. His research interests are Optoelectronics(LED), Power transmission and Automation equipment. He can be contacted at email: le.px@vlu.edu.vn

Scopus: Le Phan Xuan phanxuanle.ts@gmail.com

ID Google scholar:

<https://scholar.google.com/citations?hl=vi&user=e6QPpLEAAAAJ>

The scopus id:

<https://www.scopus.com/authid/detail.uri?authorId=57200312062>